

Development of monocular video deflectometer based on inclination sensors

Shuo Wang^{1a}, Shuiqiang Zhang^{2b}, Xiaodong Li^{1c}, Yu Zou^{3d} and Dongsheng Zhang^{*1,4}

¹Shanghai Institute of Applied Mathematics and Mechanics,
School of Mechanics and Engineering Science, Shanghai University, Shanghai, 200444, China

²School of Engineering, Huzhou university, Huzhou 313000, China

³Wuhan Sinorock Technology Co., Ltd, Wuhan, 430074, China

⁴Shanghai Key Laboratory of Mechanics in Energy Engineering, Shanghai 200072, China

(Received May 31, 2019, Revised August 7, 2019, Accepted August 26, 2019)

Abstract. The video deflectometer based on digital image correlation is a non-contacting optical measurement method which has become a useful tool for characterization of the vertical deflections of large structures. In this study, a novel imaging model has been established which considers the variations of pitch angles in the full image. The new model allows deflection measurement at a wide working distance with high accuracy. A monocular video deflectometer has been accordingly developed with an inclination sensor, which facilitates dynamic determination of the orientations and rotation of the optical axis of the camera. This layout has advantages over the video deflectometers based on theodolites with respect to convenience. Experiments have been presented to show the accuracy of the new imaging model and the performance of the monocular video deflectometer in outdoor applications. Finally, this equipment has been applied to the measurement of the vertical deflection of Yingwuzhou Yangtze River Bridge in real time at a distance of hundreds of meters. The results show good agreement with the embedded GPS outputs.

Keywords: vertical deflection; monocular vision; digital image correlation; pitch angle

1. Introduction

Large structures and infrastructure systems such as bridges, tunnels, and high buildings, have become an important symbol of civilization and have brought great convenience to industries and lives of human beings. The health surveillance plays a key role in understanding the performances of structures in construction, service and maintenance, and it helps to identify failures at an early stage. Deflections at certain positions of a large structure are often used as characteristic parameters in health monitoring. The linear variable differential transformer (LVDT) is a highly sensitive transducer for displacement measurement in a certain direction (Nassif *et al.* 2005, Hidayat *et al.* 2018, De *et al.* 2003, Lin *et al.* 2006). As it requires a solid base for supporting during the measurement, applications of this sensor are largely limited. Global positioning system (GPS) sensors are easy to use and able to measure displacement in all directions while errors in vertical direction are usually larger than those in the horizontal plane and must be considered (Merkle *et al.* 2004,

Psimoulis *et al.* 2013, Wang *et al.* 2016). Theodolites which integrate a telescopic sight for establishing horizontal and vertical angles can measure the displacement of an object at a long distance (Tang *et al.* 2019, Brown *et al.* 2015). The manual operation has become a headache especially in the condition when multiple targets are needed to measure in a short period.

Optical techniques have unique advantages for shape and deformation measurements (Su *et al.* 2016, Xu *et al.* 2017, Liu *et al.* 2019, Cai *et al.* 2016). With the development of digital image correlation (DIC), attempts have been made to apply this technology to remote displacement measurement. So far, video deflectometers have been applied to some engineering problems. For example, Ye *et al.* (2013) developed a dynamic displacement measurement system based on pattern matching. A vision-based system for multi-point structural dynamic displacement measurement was developed (Ye *et al.* 2016). Algorithms considering the influence of illumination and vapor were explored (Ye *et al.* 2016). Feng *et al.* (2015) developed a targetless non-contact measurement system for characterization of dynamic displacement of railway bridges. Xu *et al.* (2018) utilized a home-made binocular vision system to measure the deck deformation and cable vibration of a cable-stayed footbridge under pedestrian loading. In these applications, it was found that the vision system was placed roughly in the horizontal plane to capture images at a far distance. The vertical deflection on the object was proportional to the image displacement before and after loading. As indicated

*Corresponding author, Professor
E-mail: donzhang@staff.shu.edu.cn

^a M.S. Student

^b Ph.D.

^c M.S. Student

^d Senior Engineer

by Feng *et al.* (2015), the effect of the elevation angle of the vision system must be considered if a larger pitch angle occurs between the object and the observation station. Recently, Pan *et al.* (2016) proposed an imaging model which allows off-axis measurement for vertical displacement by capturing images from a far distance (Pan *et al.* 2016). A camera was assembled onto a theodolite and aligned with the telescope so that the orientation of the optical axis of the camera was known. By measuring the distance of the target with a laser rangefinder, the vertical displacement of the target can be calculated. However, since the positions to be analyzed on the large structure are usually not in the same plane parallel to the image plane, the variations of pitch angles at an individual position should also be considered in order to improve the accuracy in field test.

In this work we propose a novel imaging model based on the pinhole model which considers the variations of pitch angles in full field. Experimental study showed that the proposed model can greatly improve the accuracy of measurement. A novel monocular deflectometer is developed with the use of an inclination sensor. Illustrations are provided indicating that this layout is convenient to operate in outdoor applications.

2. Materials and methods

2.1 Deflection calculation

In engineering applications, a monocular deflectometer can be placed at an arbitrary pose facing a large structure. In such conditions, two angles which are related to the camera pose have to be introduced. One is the roll angle, defining the rotation of camera about the optical axis, which is often used to identify whether the x axis of the image coordinate is parallel to the horizontal line. The other is the pitch angle, defining the angle between the optical axis of camera and the horizontal plane.

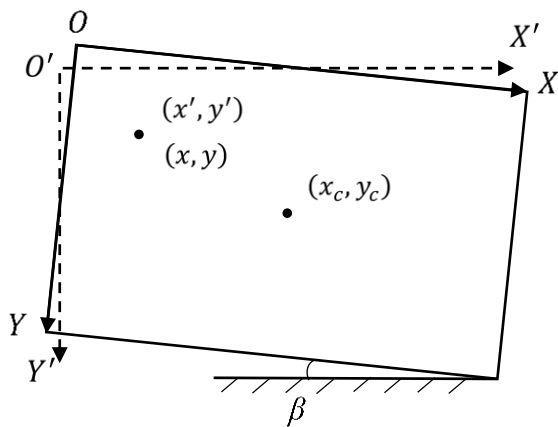


Fig. 1 Schematic figure of the image coordinate

These two angles are critical to the measurement of the monocular deflectometer. In Pan's model, the roll angle of the camera must be adjusted to zero by tuning the theodolite and the pitch angle of the camera is measured with the laser rangefinder. By assuming the pitch angle is a constant all over the image, the deflection of point on the remote object is derived (Pan *et al.* 2016). However, this assumption is questionable since the optical lines which do not pass through the optical center may have different pitch angles. In this study, we develop a model with consideration of variations of the roll and pitch angles.

The effect of the roll angle is first considered. As shown in Fig. 1, the camera is rotated about the optical center (x_c, y_c) such that the image axis OX does not coincide with the horizontal axis. Assume the image axis without rotation to be $O'X'$ and the rotation angle to be β , the relationship between (x, y) and (x', y') can be expressed as

$$\begin{bmatrix} x \\ y \\ 1 \end{bmatrix} = M \times \begin{bmatrix} x' \\ y' \\ 1 \end{bmatrix} \quad (1)$$

In the above equation, M is a 3×3 rotation matrix given as

$$M = \begin{bmatrix} 1 & 0 & x_c \\ 0 & 1 & y_c \\ 0 & 0 & 1 \end{bmatrix} \begin{bmatrix} \cos \beta & -\sin \beta & 0 \\ \sin \beta & \cos \beta & 0 \\ 0 & 0 & 1 \end{bmatrix} \begin{bmatrix} 1 & 0 & -x_c \\ 0 & 1 & -y_c \\ 0 & 0 & 1 \end{bmatrix} \quad (2)$$

$$= \begin{bmatrix} \cos \beta & -\sin \beta & (1 - \cos \beta)x_c + y_c \sin \beta \\ \sin \beta & \cos \beta & (1 - \cos \beta)y_c - x_c \sin \beta \\ 0 & 0 & 1 \end{bmatrix}$$

Thus the coordinate without rotation (x', y') can be calculated based on the results from the rotated image coordinates (x, y) , shown as follows.

$$\begin{bmatrix} x' \\ y' \\ 1 \end{bmatrix} = M^{-1} \times \begin{bmatrix} x \\ y \\ 1 \end{bmatrix} \quad (3)$$

M^{-1} is a 3×3 rotation matrix given as

$$M^{-1} = \begin{bmatrix} \cos \beta & \sin \beta & (1 - \cos \beta)x_c - y_c \sin \beta \\ -\sin \beta & \cos \beta & (1 - \cos \beta)y_c + x_c \sin \beta \\ 0 & 0 & 1 \end{bmatrix} \quad (4)$$

In consideration of the pitch angle, the schematic diagram is shown in Fig.2 with the assumption that the roll angle is equal to zero. Define OO' as the optical axis which forms a pitch angle α , and $q_0(x_0, y_0)$ as the projection in the image plane of the point Q_0 on a remote object. According to the definition, the pitch angle α_0 at q_0 is a function of the image coordinates (x_0, y_0) . The corrected pitch angle α_0 at q_0 can be derived according to the geometric relationship.

$$\alpha_0 = \tan^{-1} \left(\frac{(y_c - y_0)l_{ps}}{\sqrt{(x_c - x_0)^2 l_{ps}^2 + f^2}} \right) + \tan^{-1} \left(\frac{f \times \tan \alpha}{\sqrt{(x_c - x_0)^2 l_{ps}^2 + f^2}} \right) \quad (5)$$

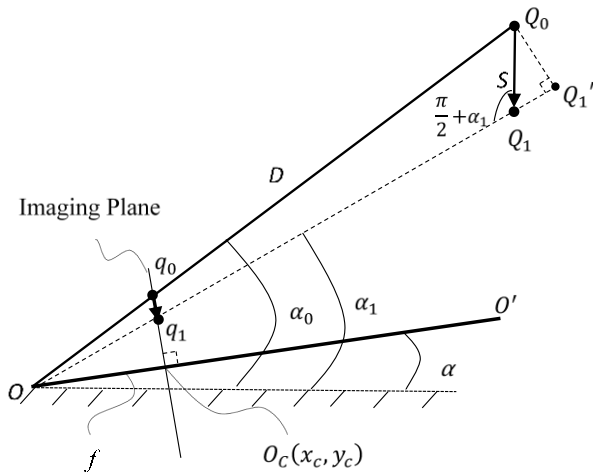


Fig. 2 Schematic figure of the vertical deflection measurement

In the above equation, l_{ps} is the physical size of the CCD array, and f is the focal length of the camera lens. In a general situation where there are a non-zero roll angle β and a pitch angle α in the monocular vision system, the actual pitch angle at an arbitrary location (x_0, y_0) in the image can be expressed as follows

$$\alpha_0' = \tan^{-1} \left(\frac{(y_c - y_0') l_{ps}}{\sqrt{(x_c - x_0')^2 l_{ps}^2 + f^2}} \right) + \tan^{-1} \left(\frac{f \times \tan \alpha}{\sqrt{(x_c - x_0')^2 l_{ps}^2 + f^2}} \right) \quad (6)$$

where the rotated image coordinate (x_0', y_0') are estimated according to Eq. (3). This equation indicates that the actual pitch angle α_0' in the captured image via a monocular vision system can be calculated based on the pitch angle of the camera optical axis α , the focus length f , the physical size of CCD array l_{ps} , and the coordinates (x_0, y_0) . As the image center (x_c, y_c) and the physical size of CCD array l_{ps} are fixed when an imaging system is selected, the actual pitch angle α_0' varies with the coordinates (x_0, y_0) and the focus length f . In Eq. (5) or (6), the first term describes the influence caused by the difference between y_c and y_0 , while the denominator in the equation determines the contribution of the focus length with respect to variations of the pitch angle. Intuitively, a large difference between y_c and y_0 causes big variations in pitch angle, and the use of a lens with short focus length could be more obvious in this situation.

During deflection measurements for large structures, the 2D image acquired with a monocular imaging system is related to a 3D object. The vertical displacement of the object can only be measured if the magnification number, the pixel displacement and the pitch angle are known. The magnification number of the imaging system is determined with the focus length and the physical size of CCD array. Therefore, the vertical displacement of the object can be calculated if the displacement of the object in the image

(pixel displacement) is determined with known pitch angle. Pan *et al.* (2016) derived an equation for calculating vertical displacement from the known pixel displacement assuming the pitch angle is constant in the full image. In this study, an accurate expression for vertical displacement calculation has been derived on the basis that the pitch angle is a function of image coordinates. In Fig. 2, if a vertical displacement occurs at the point Q_0 on the remote object, which leads to a pixel displacement from $q_0(x_0, y_0)$ to $q_1(x_1, y_1)$, the corresponding pitch angle changes from α_0 to α_1 , where α_1 is calculated according to Eq.(5) by replacing (x_0, y_0) with (x_1, y_1) . Thus, the vertical displacement S of a point Q_0 on the object is measured with the following expression, where D is the distance between the imaging system and the remote object, which can be measured with a laser rangefinder.

$$S = \frac{D \sin(\alpha_0 - \alpha_1)}{\cos \alpha_1} \quad (7)$$

In a more sophisticated situation where both the roll angle and pitch angle are considered, the vertical deflection of the object is derived.

$$S = \frac{D \sin(\alpha_0' - \alpha_1')}{\cos \alpha_1'} \quad (8)$$

In the above equation, α_1' is calculated with Eq. (6) by substituting (x, y) with (x_1, y_1) in Eq. (3). And the working distance D , i.e. the distance from the camera to the target on the structures surface, is measured by a laser range finder. A typical precision of the inclinometer sensor can reach 0.01° . This is good enough for engineering measurements (Pan *et al.* 2016). The laser range finder is a common device for distance measurements with precision varying with distance, typically 0.1m @ 100 m and 1 m @ 500 m. Therefore, the errors caused by both, the inclinometer sensor and laser rangefinder, are neglected in this study.

2.2 System configuration

Based on the developed model for vertical deflection measurement, a monocular deflectometer can be formed with a video camera combined with an aligned inclination sensor. The inclination sensor possesses abilities of perception of the inclinations in two axes. The inclination sensor is attached to the camera so that one axis agrees with the optical axis of the camera and the other axis is parallel to the x axis of the CCD array. In this layout, the inclination sensor provides information about the roll angle and the pitch angle of the optical axis in realtime. In practice, a monochrome camera (DAHENG IMAGING, Beijing, China) was selected. The camera was able to capture images in a spatial resolution of 2048×1536 pixels with 256 greyscales at a rate of 60 fps. An inclination sensor (MSENSOR TECHNOLOGY, Wuxi, China) with measuring range of $\pm 90^\circ$ and accuracy of 0.01° was mounted on the same plate as the camera and aligned with the optical axis of the camera. An iron shell was manufactured to ensure usage of the equipment in outdoor applications, as shown in Fig. 3. Digital images are

Table 1 Test parameters

f (mm)	Pitch Angle	Measuring Distance (m)						
		$P1$	$P2$	$P3$	$P4$	$P5$	$P6$	$P7$
5	25°24'	1.290	1.165	1.075	1.000	0.930	0.880	0.860
16	21°30'	2.031	1.918	1.932	1.886	1.840	1.837	1.808
25	21°30'	1.946	1.914	1.896	1.863	1.836	1.820	1.795



Fig. 3 The video deflectometer for large-scale structure

transmitted to a laptop via a USB3.0 cable and processed with the specifically designed DIC software.

In order to achieve a realtime output for vertical deflection measurement, a fast DIC scheme has been adopted (Wu *et al.* 2016). This algorithm divides the calculation into two domains, i.e. in the integer and subpixel domains. In the integer domain, an efficient search scheme with combination of an improved particle swarm optimization algorithm and the gradient descent search algorithm achieves an efficient and robust convergence near the true value. Inverse compositional Gauss-Newton (IC-GN) algorithm (Gao *et al.* 2015, Su *et al.* 2018, Pan *et al.* 2013) is normally used to achieve fast, robust, and accurate subset matching. Combined with the inverse compositional Gauss-Newton (IC-GN) algorithm for subpixel registration and the CPU parallel computing technology, this real-time DIC algorithm could reach an accuracy of 0.005 pixels when a cubic B-spline interpolation is used.

Prior to the measurement, the roll and pitch angles are fetched through a parallel port and the individual distance of points of interest on the large structure are measured with a laser rangefinder. The vertical deflections up to 8 locations are output at a rate of 40 Hz.

3. Experiments

3.1 laboratory test

In order to demonstrate the influence of pitch angle on the accuracy of vertical deflection measurement, a laboratory study was carried out. A series of markers, $P1$, $P2$, ... and $P7$, were attached onto a rigid bar which was installed vertically on a precision translation stage, as shown in Fig.4. A camera combined with an aligned inclination sensor acquired images before and after

translation. During the experiments, three prime lenses with focus length of 5 mm, 16 mm, and 25 mm were used. The pan/tilt unit was adjusted to allow roll angle equal to zero. The pitch angle of the optical axis of the camera was measured before each test. Seven markers on the vertical bar were selected as the points of interest. The corresponding distances to the camera were measured with a precision laser rangefinder (MILESEEY, Shenzhen, China), respectively. All test parameters are listed in Table 1.

During the experiments, the translation stage was adjusted to move vertically with displacements at 1.75 mm, 3.5 mm, and 5.25 mm, respectively. The camera acquired the live images and output the vertical displacement simultaneously. In order to evaluate the importance of variations of the pitch angle, the vertical displacement was calculated based on the fixed pitch angle (Pan *et al.* 2016) and the proposed model. As indicated in the left column of Fig. 5, the seven selected points gave different vertical displacement outputs. With the proposed model, the vertical displacement outputs were uniform over the entire image (right column in Fig. 5).

3.2 Field test

The developed monocular deflectometer was used in a field test. The target was a marker which was attached to a precision translation stage, as shown in Fig. 6. The device was fixed on a vibration-isolated table and placed on the roof of a building with height about 13 m. The developed deflectometer was set up on the ground with a stable tripod. The distance to the target was measured with the precision laser rangefinder as 21.1 m.

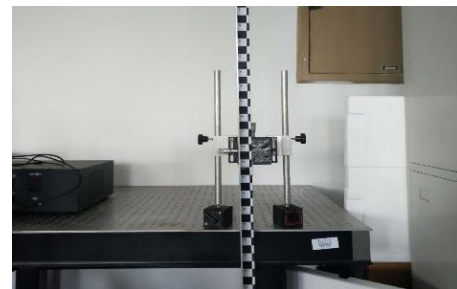


Fig. 4 Markers attached to a bar mounted on a precision translation stage

Table 2 Field test conditions

Image Coordinate	Pitch Angle	Roll Angle
(1038,221)	35°46'	2°59'
(1038,763)	37°54'	3°09'
(1038,1210)	39°40'	3°16'

Table 3 Results of field test

Image Coordinate	Prescribed Displacement (mm)	Uniform Pitch Angle		Proposed Method	
		Average (mm)	RMSE (mm)	Average (mm)	RMSE (mm)
(1038,221)	3.500	3.399	0.115	3.501	0.047
(1038,763)	3.500	3.535	0.053	3.544	0.053
(1038,1210)	3.500	3.573	0.112	3.494	0.067

In order to evaluate the convenience and accuracy of the developed device, the deflectometer was placed at multiple poses as long as the target was clearly enclosed in the image. In these situations, the pitch angle of the camera optical axis and the roll angle were different, as shown in Table 2. Prior to the measurement, the roll and pitch angles were collected with the inclination sensor. In the experiment, the translation stage was adjusted to produce a vertical displacement of 3.50 mm. Seven measurements were conducted in each camera pose. The average readouts are presented in Table 3, in comparison with the method based on uniform pitch angle.

3.3 Bridge test

The developed deflectometer was used to monitor the dynamic vertical deflections at certain locations on the Yingwuzhou Yangtze River Bridge, Wuhan, China. This bridge is the largest suspension bridge with three towers and four spans in the world. The deflectometer was placed at the west side of the Yangtze River to measure the dynamic deflections at certain locations between the second and third spans which are 850 m apart, as shown in Fig. 7.

There are GPS sensors embedded in this super large bridge. The dynamic deflection readouts are collected via the 4G communication channels with a frequency of 1/4 Hz. To verify the utility of the deflectometer, its outputs were compared with the GPS signals. As shown in Fig. 7, the deflectometer was deployed with cable links to a laptop. The device was powered with a DC-AC inverter. Three locations near the embedded GPS sensors were selected as the targets. The distances were measured with a ranging telescope (SNDWAY, Shenzhen, China) as 267 m, 400 m, and 520 m away from the deflectometer, respectively. The lens with focus length $f = 50$ mm was chosen to measure the target at distance of 267 m. Then the lens with focus length $f = 75$ mm was chosen to measure the targets at further distances. During the dynamic test, the first image was taken as the reference and the relative vertical displacement was calculated from the following images based on the proposed model. The vertical displacement variations

resulted from the deflectometer and GPS sensors are shown in Fig. 8.

4. Discussions

The laboratory experiments illustrate the significance of variations of the pitch angle on the accuracy of the measurement. The pitch angle obtained from the inclination sensor is considered as the angle at the image center if it is aligned with the optical axis of the camera. In the experiment, the selected markers were distributed with large differences in y coordinate. It was found that the vertical displacements output from these markers were varied with the positions of the markers. Errors increase with the distance to the image center. Thus, it is necessary to calculate the actual pitch angle according to the image coordinates with the proposed model. In Fig. 9, the root mean square error (RMSE) of the vertical displacement outputs are plotted versus the y coordinates in cases where three kinds of prime lens are used. As evident, the proposed model provides an accurate solution for vertical deflection measurement with a monocular vision system.

The variations of the pitch angle in the image are also a function of the focus length of the imaging system. As indicated in Fig. 9, errors introduced by the change of the pitch angle over the image reduce with the focus length. Therefore, it is critical to consider this error if the vertical displacement of a large structure is measured in a close range. Nevertheless, at a far distance with the use of a lens having long focus length, the small error in pixel caused by the pitch angle might be magnified due to the increase of working distance.

The developed monocular deflectometer combines a video camera with a two-axis inclination sensor. One axis of the sensor is carefully aligned with the optical axis of the camera and the other is parallel to the x axis of the CCD array. The pitch and roll angles of the image center are collected in realtime. The vertical displacement of the remote object can be accurately calculated based on the proposed model with this layout. The benefit of this layout

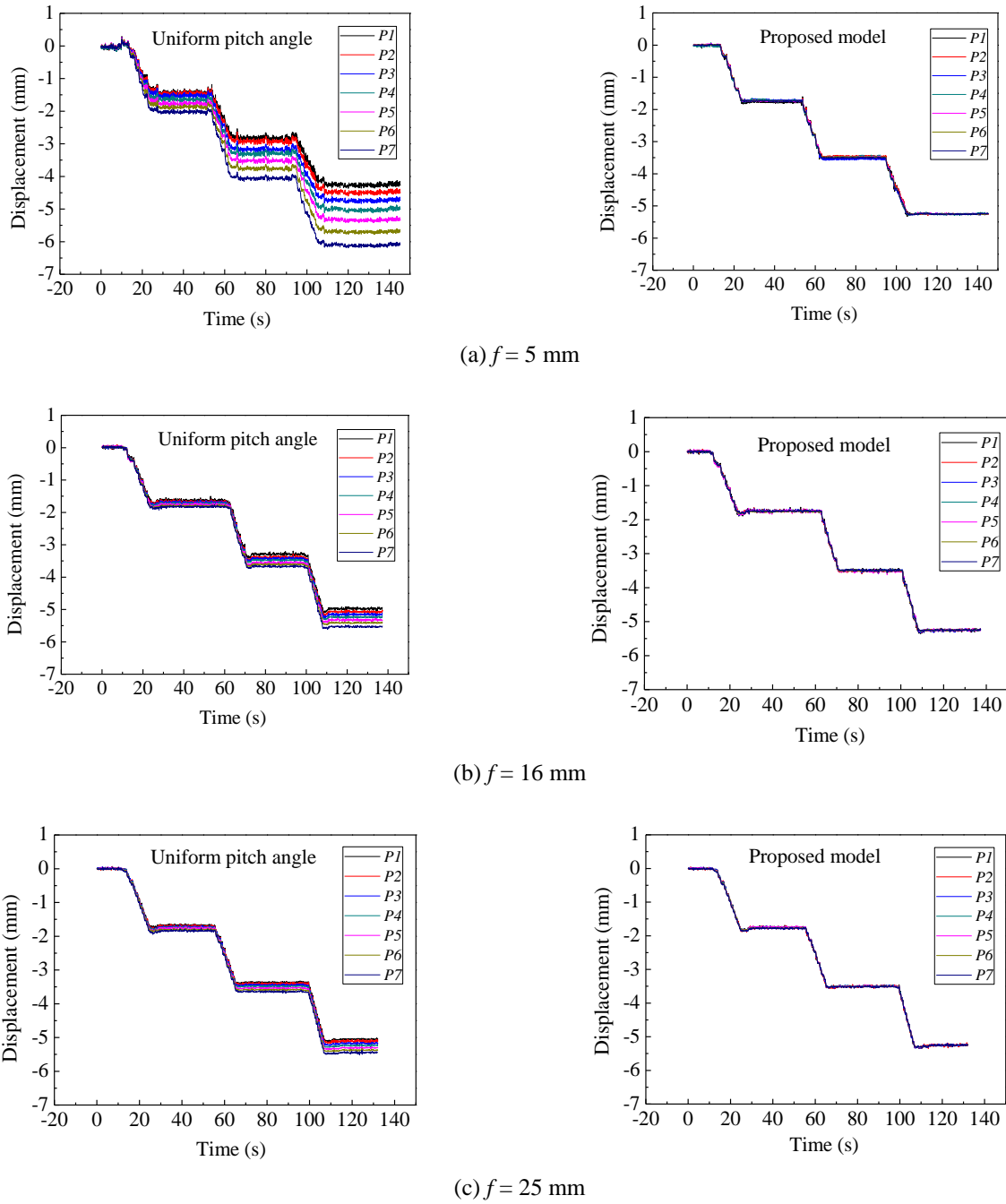


Fig. 5 Results of vertical movements



Fig. 6 Marker attached to a precision translation stage



Fig. 7 Bridge test setup

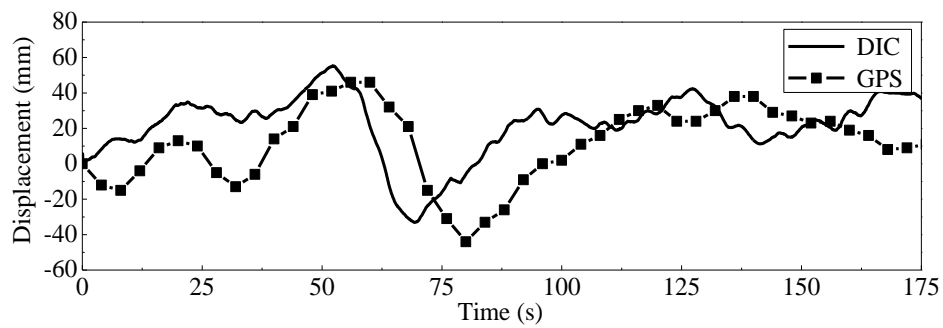
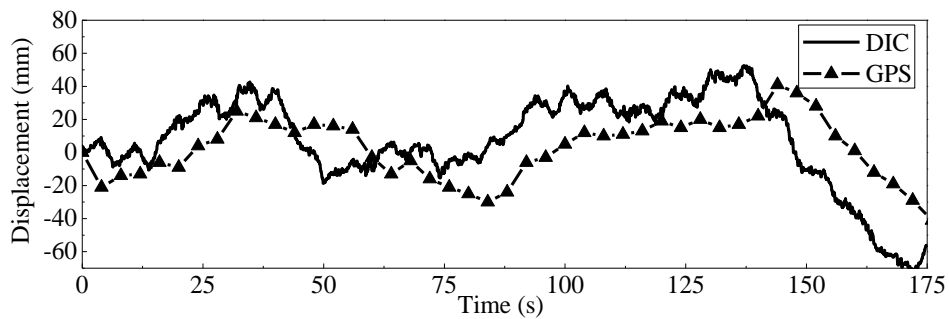
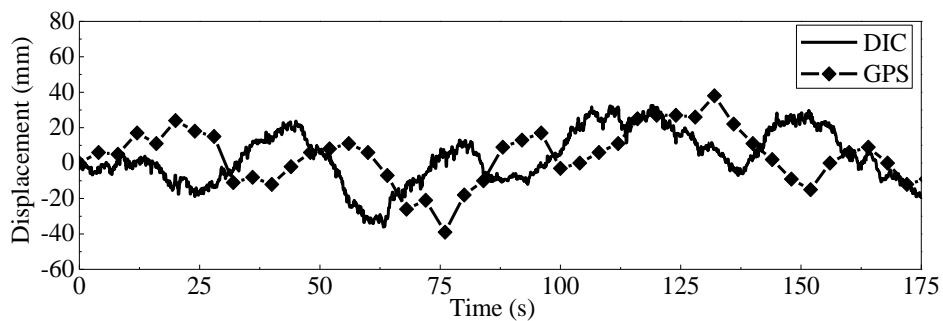
(a) $f = 50$ mm, Distance = 267 m(b) $f = 75$ mm, Distance = 400 m(c) $f = 75$ mm, Distance = 520 m

Fig. 8 Deflections of the bridge

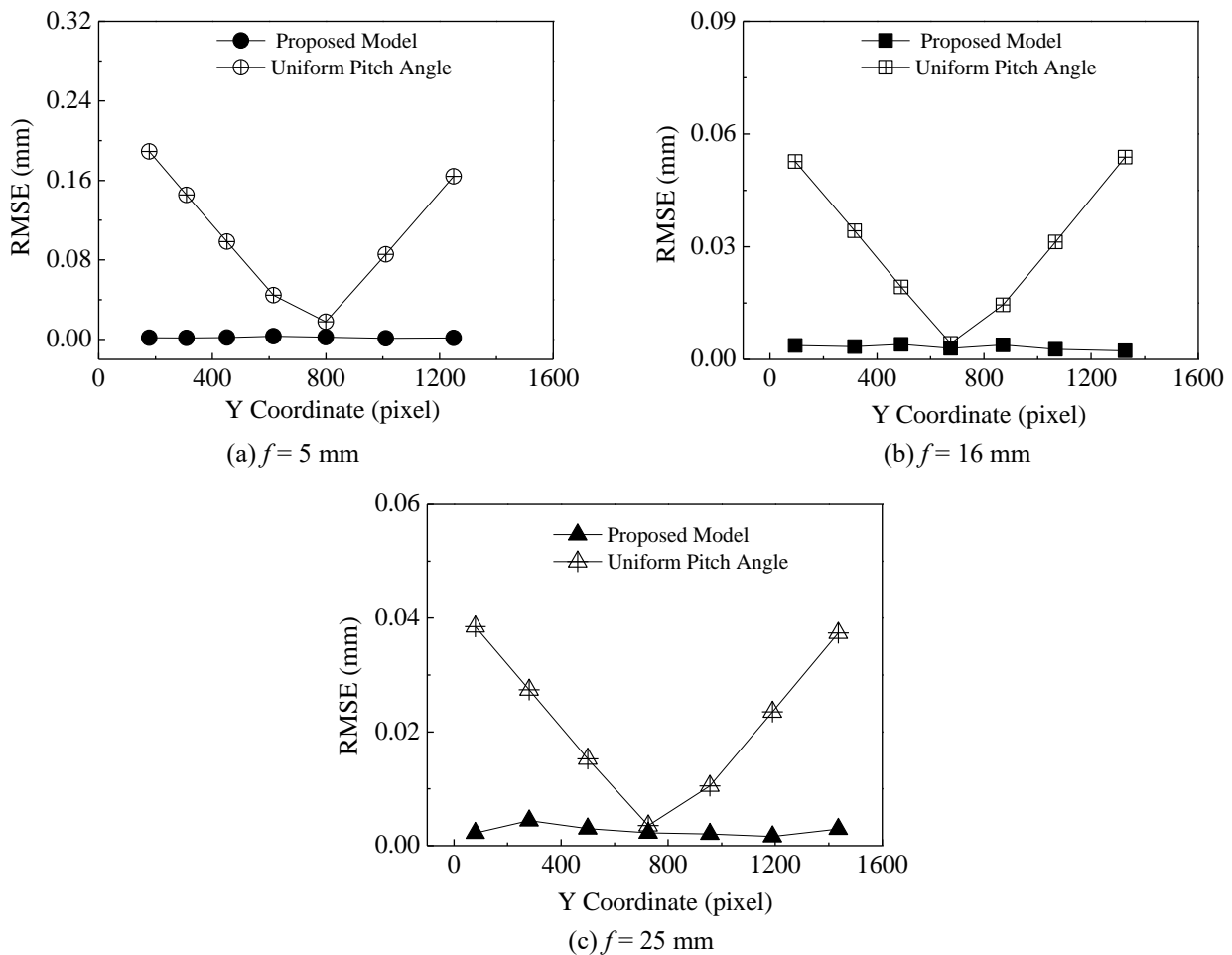


Fig. 9 RMSE with multiple focus lengths

also lies in the operation of the device. It does not need to use a theodolite to carefully find the horizontal plane. The experimental results listed in Table 3 demonstrate that accurate measurements can be achieved as long as a clear image is acquired regardless of the roll and pitch angles of the camera axis.

A good attempt has been made to apply this monocular deflectometer to the dynamic deflection measurement of a large bridge. Although the resultant deflection curves do not closely match the signals given by the GPS sensors, the amplitudes are in the same level and the trend in displacement is the same. Note that these two measurement systems are independent of each other and a time delay between the displacement curves is reasonable. In this regard, the developed monocular deflectometer has had a fairly good performance in the remote measurements. In Fig. 8, one may notice that when the working distance increases from 267 m to 520 m, the noise in the displacement output increases appreciably. The noise may come from many aspects such as ambient vibration of the deflectometer base produced by moving vehicles or wind, and vapor effect over the river (Tian *et al.* 2016, Ye *et al.* 2015, Martins *et al.* 2013, Martins *et al.* 2015) or heat haze

(Luo *et al.* 2017). Ambient vibration of the deflectometer base leads to camera movement which causes remarkable errors in measurements. A common routine for eliminating such errors is to find a stationary object in the image as a reference (Luo *et al.* 2018, Yoneyama 2007). In the meantime, the inclination sensor is able to collect the camera pose in realtime. It is possible to identify apparent changes in pitch and roll angles of the camera during measurement. This helps to eliminate errors of camera movement. However, the accuracy of the inclination sensor limits the abilities for noise depression. The vapor or heat haze is another concern for remote deflection characterization. It ruins the image quality and accordingly adds noise to the measurement (Ye *et al.* 2016). Algorithms for image filtering and novel image matching have been developed to improve the accuracy (Luo *et al.* 2018, Luo *et al.* 2017). Methods for using LED targets are also proposed to overcome the difficulty in imaging at far distances (Tian *et al.* 2016). All these efforts are helpful towards accurate deflection measurements using video deflectometers.

5. Conclusions

In this study, the influence of variations of the pitch angle in the image has been considered for vertical displacement measurement using a monocular vision system.

- It is found that errors increase with the distance to the image center. A novel model for calculating vertical deflection of a remote object using a monocular vision system has been proposed. With the information about the roll and pitch angles of the optical axis of the camera, the vertical displacement can be calculated accurately.

- A monocular video deflectometer has been developed, which consists of a video camera and a bi-axial inclination sensor. One axis of the inclination sensor is aligned with the optical axis of the camera, and the other is parallel to the x axis of the CCD array. This layout enables real time collection of the roll and pitch angles at the image center. It simplifies the operation for finding the horizontal plane and suitable for field tests. Combined with a robust DIC algorithm, this device can achieve a fast and robust measurement in outdoor applications.

Acknowledgments

The authors would like to thank the support from the National Key R&D Program of China # 2018YFF01014200, National Natural Science Foundation of China through grants #11727804, #51732008 and #11672347 for supporting this work.

References

- Brown, C.J., Roberts, G.W., Atkins, C., Meng, X. and Colford, B. (2015), "Deflections and frequency responses of the forth road bridge measure by GPS", *Thomas Telford*, **2015**, 479-486.
- Cai, Y.L., Yang, S.L., Wang, Y.H., Fu, S.H. and Zhang, Q.C. (2016), "Characterization of the deformation behaviors associated with the serrated flow of a 5456 Al-based alloy using two orthogonal digital image correlation systems", *Mater. Sci. Eng. A.*, **664**, 155-164. DOI: 10.1016/j.msea.2016.04.003.
- De, R.G., Xia, H., Zhang, N. and Zhang, H. (2003), "Experimental study of a prestressed trough bridge for high speed railway", *Eng. Mech.*, **20**(6), 99-105. DOI: 10.1007/s11769-003-0044-1.
- Feng, D., Feng, M.Q., Ozer, E. and Fukuda, Y. (2015), "A vision-based sensor for noncontact structural displacement measurement", *Sensors*, **2015**(15), 16557-16575. DOI:10.3390/s150716557.
- Feng, M.Q., Asce, F., Fukuda, Y., Feng, D. and Mizuta, M. (2015), "Nontarget vision sensor for remote measurement of bridge dynamic response", *J. Bridge Eng.*, **20**(12), 04015023. DOI: 10.1061/(ASCE)BE.1943-5592.0000747.
- Gao, Y., Cheng, T., Su, Y., Xu, X., Zhang, Y. and Zhang, Q. (2015), "High-efficiency and high-accuracy digital image correlation for three-dimensional measurement", *Opt. Lasers Eng.*, **65**, 73-80. DOI: 10.1016/j.optlaseng.2014.05.013.
- Hidayat, I., Suangga, M. and Maulana, M.R. (2018), "The effect of load position to the accuracy of deflection measured with LVDT sensor in I-girder bridge", *Int. Conf. Eng. Develop.*, Kanazawa, Japan, January. DOI: 10.1088/1755-1315/109/1/012024.
- Lin, M.W. (2006), "Structural deflection monitoring using an embedded ETDR distributed strain sensor", *J. Intel. Mat. Syst. Str.*, **17**(5), 423-430. DOI: 10.1177/1045389X06058631.
- Luo, L. and Feng, M.Q. (2017), "Vision based displacement sensor with heat haze filtering capability", *P. Int. Workshop Struct. Health Monit.*, Liverpool, May.
- Luo, L., Feng, M.Q. and Wu, Z.Y. (2018), "Robust vision sensor for multi-point displacement monitoring of bridges in the field", *Eng. Struct.*, **163**, 255-266. DOI: 10.1016/j.engstruct.2018.02.014.
- Liu, Y., Zhang, Q., Su, Y., Gao, Z., Fang, Z. and Wu, S. (2019), "The mechanism of strain influence on interpolation induced systematic errors in digital image correlation method", *Opt. Lasers Eng.*, **121**, 323-333. DOI: 10.1016/j.optlaseng.2019.04.023.
- Merkle, W.J. and Myers, J.J. (2004), "Use of the total station for load testing of retrofitted bridges with limited access", *Smart Mater. Struct.*, San Diego, U.S., March. DOI: 10.1117/12.539992.
- Martins, L.L., Rebordão, J.M. and Ribeiro, A.S. (2013), "Conception and development of an optical methodology applied to long-distance measurement of suspension bridge dynamic displacement", *Int. Measurement Confeder.*, Genoa, September. DOI: 10.1088/1742-6596/459/1/012055.
- Martins, L.L., Rebordão, J.M. and Ribeiro, A.S. (2015), "Structural observation of long-span suspension bridges for safety assessment: Implementation of an optical displacement measurement system", *IMEKO Sym. Measurement Sci. Safe. Sec.*, Funchal, September. DOI: 10.1088/1742-6596/588/1/012004.
- Nassif, H.H., Gindy, M. and Davis, J. (2005), "Comparison of laser Doppler vibrometer with contact sensors for monitoring bridge deflection and vibration", *NDTE. Int.*, **38**(3), 213-218. DOI: 10.1016/j.ndteint.2004.06.012.
- Pan, B., Li, K. and Tong, W. (2013), "Fast, robust and accurate digital image correlation calculation without redundant computations", *Exp. Mech.*, **53**(7), 1277-1289. DOI: 10.1007/s11340-013-9717-6.
- Psimoulis, P.A. and Stiros, S.C. (2013), "Measuring deflections of a short-span railway bridge using a robotic total station", *J. Bridge Eng.*, **18**(2), 182-185. DOI: 10.1061/(ASCE)BE.1943-5592.0000334.
- Pan, B., Tian, L. and Song, X. (2016), "Real-time, non-contact and targetless measurement of vertical deflection of bridges using off-axis digital image correlation", *NDTE. Int.*, **2016**(79), 73-80. DOI: 10.1016/j.ndteint.2015.12.006.
- Su, Y., Zhang, Q., Xu, X. and Gao, Z. (2016), "Quality assessment of speckle patterns for DIC by consideration of both systematic errors and random errors", *Opt. Lasers Eng.*, **86**, 132-142. DOI: 10.1016/j.optlaseng.2016.05.019.
- Su, Y., Zhang, Q., Xu, X., Gao, Z. and Wu, S. (2018), "Interpolation bias for the inverse compositional Gauss-Newton algorithm in digital image correlation", *Opt. Lasers Eng.*, **100**, 267-278. DOI: 10.1016/j.optlaseng.2017.09.013.
- Tian, L. and Pan, B. (2016), "Remote bridge deflection measurement using an advanced video deflectometer and actively illuminated led targets", *Sensors*, **16**(9), 1344. DOI: 10.3390/s16091344.
- Tian, Y. and Fang, M. (2016), "A time synchronization method for inertial sensor and visual sensor", *P. Intell. Control Autom.*, Guilin, June. DOI: 10.1109/WCICA.2016.7578516.
- Tang, X., Li, X., Robert, W.G. and Hancock, M.C. (2019), "1 Hz GPS satellites clock correction estimations to support high-rate dynamic PPP GPS applied on the Severn suspension bridge for deflection detection", *GPS Solut.*, **2019**(2), 23-28. DOI: 10.1007/s10291-018-0813-z.
- Wang, J., Meng, X., Qin, C. and Yi, J. (2016), "Vibration

- frequencies extraction of the forth road bridge using high sampling GPS data”, *Shock Vib.*, **2016**(2), 1-18. DOI: 10.1155/2016/9807861.
- Wu, R., Kong, C., Li, K. and Zhang, D. (2016), “Real-time digital image correlation for dynamic strain measurement”, *Exp. Mech.*, **56**(5), 833-843. DOI: 10.1007/s11340-016-0133-6.
- Xu, X., Su, Y. and Zhang, Q. (2017), “Theoretical estimation of systematic errors in local deformation measurements using digital image correlation”, *Opt. Lasers Eng.*, **88**, 265-279. DOI: 10.1016/j.optlaseng.2016.08.016.
- Xu, Y., Brownjohn, J. and Kong, D. (2018), “A non-contact vision-based system for multipoint displacement monitoring in a cable-stayed footbridge”, *Struct. Control Health Monit.*, **25**(5), e2155. DOI: 10.1002/stc.2155.
- Yoneyama, S. (2007), “Bridge deflection measurement using digital image correlation”, *J. JSEM.*, **7**(1), 34-40. DOI: 10.1111/j.1747-1567.2006.00132.x.
- Ye, X.W., Ni, Y.Q., Wai, T.T., Wong, K.Y., Zhang, X.M. and Xu, F. (2013), “A vision-based system for dynamic displacement measurement of long-span bridges: algorithm and verification”, *Smart. Struct. Syst.*, **12**(3-4), 363-379. http://dx.doi.org/10.12989/sss.2013.12.3_4.363.
- Ye, X.W., Yi, T.H., Dong, C.Z., Liu, T. and Bai, H. (2015), “Multipoint displacement monitoring of bridges using a vision-based approach”, *Wind Struct.*, **20**(2), 315-326. <http://dx.doi.org/10.12989/was.2015.20.2.315>.
- Ye, X.W., Dong, C.Z. and Liu, T. (2016), “Image-based structural dynamic displacement measurement using different multi-object tracking algorithms”, *Smart. Struct. Syst.*, **17**(6), 935-956. <http://dx.doi.org/10.12989/sss.2016.17.6.935>.
- Ye, X.W., Yi, T.H., Dong, C.Z. and Liu, T. (2016), “Vision-based structural displacement measurement: system performance evaluation and influence factor analysis”, *Measurement*, **2016** (88), 372-384. DOI: 10.1016/j.measurement.2016.01.024.